Journal of the European Ceramic Society **10** (1992) 437–452

Dielectric Ceramics with Relaxors and a Tetragonal Tungsten Bronze

J. M. Haussonne,[a] G. Desgardin,[b] A. Herve[a] & B. Boufrou[b]

[a]France Telecom, CNET LAB/OCM/TAC, BP40, 22301, Lannion Cedex, France
[b]ISMRa Laboratoire CRISMAT, University of Caen, Campus II, 14050 Caen Cedex, France

(Received 7 October 1991; revised version received 23 January 1992; accepted 26 February 1992)

Abstract

Type II ferroelectric ceramics with high dielectric constants and flat curves $\varepsilon = f(T)$ have, until now, only been obtained with oxides which exhibit the perovskite structure. Another family of oxides, the tetragonal tungsten bronze (TTB)-type niobates, should be of great interest for such applications because of their structure, which is, indeed, very closely related to that of perovskite.

The authors report here on the sintering and dielectric properties of new ceramics based on the niobate $K_{0.2}Sr_{0.4}NbO_3$ (KSN) which exhibits the TTB structure, and show how the addition of a perovskite such as a relaxor or $BaTiO_3$ or a mixture of these perovskites can lead to a dielectric material compatible with the Y7R or X7R Electronic Industries Association specifications with a dielectric constant ε as high as 6000. Moreover, the use of a lithium salt as sintering agent has been shown to be important for the elaboration of those ceramics, and particularly allows the synthesis of type I materials with a dielectric constant ε as high as 3000.

Ferroelektrische Keramiken des Typs II mit hohen Dielektrizitätskonstanten und flachem $\varepsilon = f(T)$-Verlauf werden bis heute ausschließlich aus Oxiden gewonnen, die eine Perowskit-Struktur besitzen. Eine andere Gruppe von Oxiden, und zwar Niobate des Strukturtyps tetragonaler Wolframbronze (TTB), sollte ebenfalls für die erwähnten Anwendungen nicht außer acht gelassen werden, da ihre Struktur sehr nahe mit der des Perowskits verwandt ist.

In dieser Arbeit wird über das Sintern und die dielektrischen Eigenschaften neuer Keramiken auf der Basis eines Niobates der Zusammensetzung $K_{0.2}Sr_{0.4}NbO_3$ (KSN) berichtet, das die TBB-Struktur aufweist und veranschaulicht, wie die Zugabe eines Perowskits, so wie beispielsweise ein Relaxor oder $BaTiO_3$ oder aber eine Mischung aus Perowskiten, ein dielektrisches Material ergeben kann, das den Y7R oder X7R Electronic Industries Association Spezifikationen mit einer Dielektrizitätskonstante ε von etwa 6000 genügt. Außerdem zeigt sich, daß die Verwendung eines Lithium-Salzes als Sinteragens wichtig für die Entwicklung dieser Keramiken ist und insbesondere die Synthese von Werkstoffen des Typs I mit einer Dielektrizitätskonstante ε von mindestens 3000 ermöglicht.

Les céramiques ferroélectriques de type II, présentant une constante diélectrique élevée et une courbe $\varepsilon = f(T)$ plane, ont été jusqu'à présent obtenues avec des oxydes de structure cristalline perovskite. Une autre famille d'oxydes, les niobates de structure bronze quadratique de tungstène (TTB), devrait présenter un intérêt majeur pour de telles applications car leur structure est très proche de celle de la perovskite.

On présente dans cet article le frittage et les propriétés diélectriques de nouvelles céramiques basées sur le niobiate $K_{0.2}Sr_{0.4}NbO_3$ (KSN) qui présente la structure TTB et on montre comment l'addition d'une perovskite en tantque matériau relaxateur, ou de $BaTiO_3$ ou d'un mélange de telles perovskites, peut conduire à l'obtention d'un matériau diélectrique compatible avec les spécifications Y7R ou X7R de l'Electronic Industries Association avec une constante diélectrique atteignant 6000. De plus, on montre que l'utilisation d'un sel de lithium comme additif de frittage est particulièrement efficace et permet la synthèse de matériaux de type I avec une constante diélectrique atteignant 3000.

Journal of the European Ceramic Society 0955-2219/92/$5.00

1 Introduction

Much research concerning new dielectric materials has been made in recent years. Its general theme is the obtention of low-cost reliable multilayer ceramic capacitors with a volume capacitance as high as possible. So, as well as low firing temperature dielectric compositions allowing the use of high silver concentration electrodes, high dielectric constant materials have been developed. Among these compositions, relaxor materials[1] are characterized both by low sintering temperatures (lower than 1000°C) and very high dielectric constants (higher than 35000).[2,3] However, these particular materials lead only to the Z5U or the Y5V Electronic Industries Association specifications (see Appendix). All attempts to use them for stable characteristics lead only to low dielectric constants, i.e. to non-attractive materials when considering the classical X7R $BaTiO_3$-based compositions.

It appears that up to now dielectric materials for capacitors are only obtained with oxides which exhibit the perovskite structure. Another family of oxides, the tetragonal tungsten bronze (TTB)-type niobates should be of interest for such applications.[4-6] The structure of these phases (Fig. 1) is indeed closely related to that of perovskite (Fig. 2), since it is built up of similar columns of four rows of octahedra forming, besides other tetragonal and pentagonal tunnels, four-sided tunnels[7] similar to the four-sided cavities of the perovskite structures. Furthermore, these materials are either ferro- or antiferroelectric and have, as does barium titanate, a Curie temperature. Their structure below the Curie temperature can also be described as being built in a quadratic lattice, with a quadratic distortion defined as the $\frac{c}{a} \cdot \sqrt{10}$ ratio, a and c being the lattice parameters. In the case of $BaTiO_3$, the quadratic distortion defined as the c/a ratio is close to 1, and its particular dielectric properties are closely related to that. So similar properties are logically expected in the case of the TTB structures when considering their $\frac{c}{a} \cdot \sqrt{10}$ ratio. Indeed,

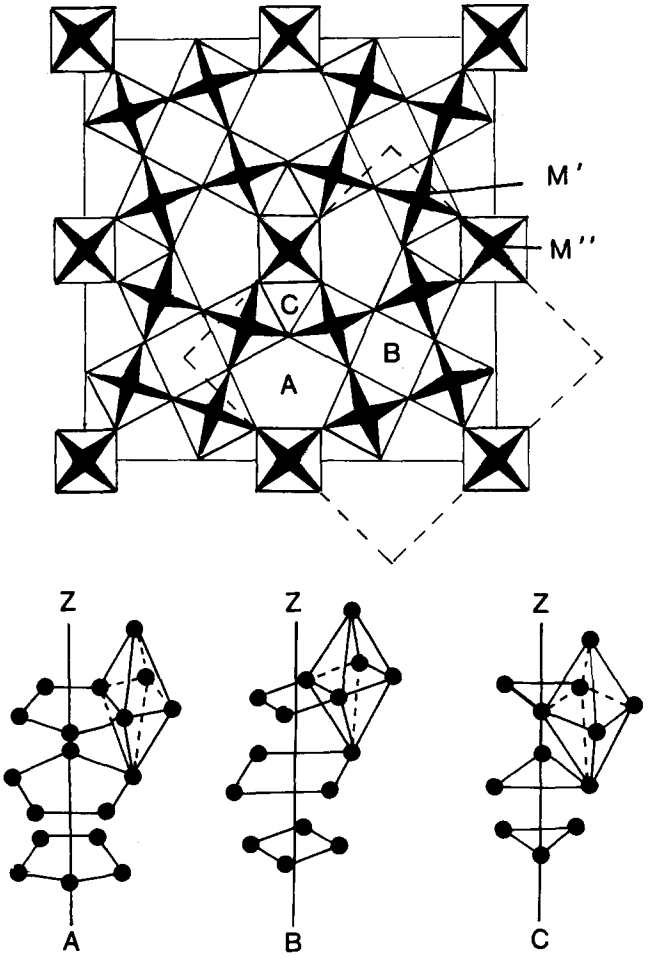

Fig. 1. The tetragonal tungsten bronze structure with the different cationic crystallographic sites.

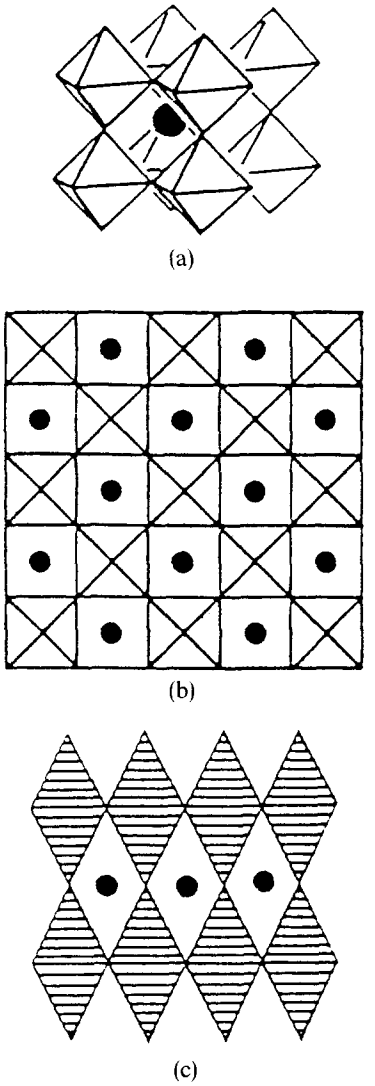

Fig. 2. The perovskite structure.

for example, $Ba_4K_2Nb_{10}O_{30}$, $Sr_4Na_2Nb_{10}O_{30}$ or $Sr_4K_2Nb_{10}O_{30}$ present a dielectric constant at room temperature higher than 1000 or 2000°C, and a Curie temperature respectively of 302, 192 and 160°C where the dielectric constant increases. Therefore, the idea is to transform these materials by substitutions and creation of ceramics with inhomogeneous phases in the same manner as has been done with classical dielectric compositions based on barium titanate. So the authors present here their first results obtained when one TTB structure, the strontium potassium niobate, was associated with different perovskite compounds to promote during sintering an inhomogeneous solid solution between them, or a microstructure made of mixed phases, with the consequence of only a little temperature dependence of the dielectric constant.

A patent has been published that describes such new dielectric ceramics sintered from a powder, including a tetragonal tungsten bronze, and relaxor materials.[8] These ceramics are claimed to have a high dielectric constant, higher than 4000, with tenperature characteristics described by the X7R specification.[9,10] However, when exploring such new systems, the authors have also been able to sinter other dielectric materials characterized by high dielectric constants, and also by a temperature dependence that allows to describe them as type I materials (see Appendix); they are characterized by a linear temperature dependence coefficient and low losses.[11]

2 Experimental

2.1 Synthesis

The materials included in the dielectric compositions are:

—Relaxor materials that are complex perovskites having lead in their A site. Among these materials

$$0{\cdot}77Pb(Mg_{1/3}Nb_{2/3})O_3 + 0{\cdot}33Pb(Fe_{1/2}Nb_{1/2})O_3 \quad \text{(PMN–PFN)}$$

has been extensively used. The synthesis of these oxides has previously been described[12,13] and will not be detailed here.

—The tetragonal tungsten bronze $K_2Sr_4Nb_{10}O_{30}$, called KSN. This material is sometimes labelled $K_{0{\cdot}2}Sr_{0{\cdot}4}NbO_3$ in order to point out the analogy existing with the perovskite structure. It is synthesized by calcination of the stoichiometric mixture of K_2CO_3, $SrCO_3$ and Nb_2O_5, at 1200°C in air for 12 h (with a heating rate of 150°C/h).

For these two materials the oxides and carbonates used for the synthesis are Rhône-Poulenc products (purity ≥99%). The mixing is performed in wet medium (ethanol), using either an attritor (Netzch) (30 g load) or 'pulverisette' Fritsch No. 6 (15 g load). The obtained slurry is dried on 'infrared heater' and disagglomerated in an agate mortar.

—As in the case of the previous studies concerning the relaxor materials, additions of lithium in small amounts in the form of lithium carbonate or barium lithium fluoride ($BaLiF_3$) are also studied.

2.2 Sintering

After calcination, KSN, the relaxor material and the sintering agent are mixed in alcoholic medium. The dried mixture is added with an aqueous solution at 5% of a binder agent (Rhodoviol; Prolabo, Paris) at a rate of 2 drops/g. The mixture is then pressed in the form of discs of 12 mm diameter and 1 mm thickness, under 1000 kg/cm^2, using a uniaxial press. The discs are placed vertically in the grooves of an alumina support in order to minimize the contact with the support. The discs are sintered in air at a temperature ranging from 1200 to 1300°C during 1 to 4 h, with a heating rate of 150°C/h, and furnace cooled. Under these conditions, only poor weight loss was observed, especially concerning lead, which, in fact, is trapped in the perovskite and tetragonal tungsten bronze (TTB) lattices.

2.3 Characterization of ceramics

The sintered ceramics are identified by X-ray diffraction, either from powder using a Guinier camera or from discs using an X-ray powder diffractometer working with CuK_α. The microstructure is studied by scanning electron microscopy using a Jeol 840.

The electrical characterization is performed on discs whose faces are painted with the alloy In–Ga, in order to realize a capacitor; the metallization concerns only a part of the surface of the discs in order to avoid 'edge effects'. The insulation resistance measurements are made with a DC bias equal to 60 or 100 V, i.e. 0·1 V/μm. Dielectric characterizations are performed at 1 kHz.

3 Type I Ceramics

Table 1 gives the range of compositions leading to type I materials that include 0–65 mol% of KSN,

Table 1. The different compositions studied

KSN (mol%)	*PMN (mol%)*	*PFN (mol%)*	*Li_2CO_3 (mol%) (corresponding to 1 wt%)*
0	77	23	4·26
2	75	23	4·64
5	73	22	5·19
8	71	21	5·75
13	67	20	6·6
25	58	17	8·76
32	52	16	9·94
45	42	13	12·07
65	27	8	15·24

with the complement up to 100 mol% of the classical 0·77 PMN–0·23 PFN formulation. Lithium carbonate (0–2 wt%) was then added.

3.1 Sintering

The shrinkage of different materials versus sintering temperature (Figs 3 and 4) shows that the higher the KSN concentration, the more refractory the material. Also, the larger the lithium amount, the less refractory the material. In fact, considering the sintering temperatures used, it is noted that, depending on the studied material, some of them will be sintered at a temperature higher than strictly necessary for densification. Such a treatment is necessary to obtain usable properties, as will be discussed further.

Figure 5 shows the dilatometric curve recorded during the sintering cycle of a material containing 25 mol% KSN and 2 wt% lithium carbonate. In fact,

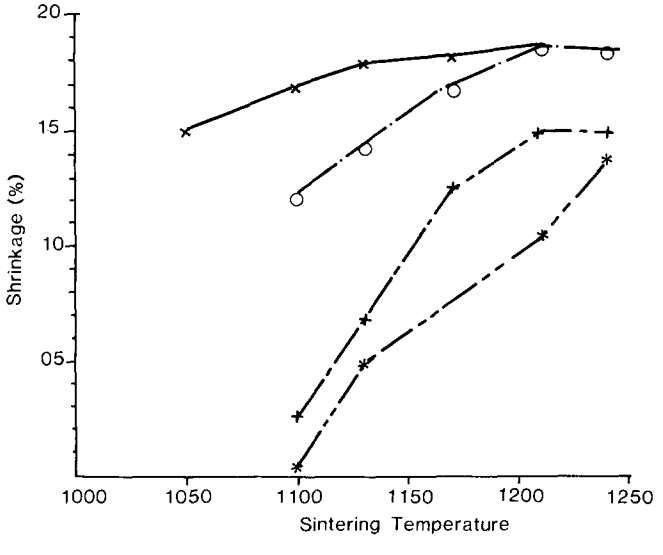

Fig. 3. Shrinkage of materials with 45 mol% KSN versus lithium carbonate amount and sintering temperature. – – – –, 0 wt% Li_2CO_3; – – –, 0·5 wt% Li_2CO_3; — · —, 1 wt% Li_2CO_3; ——, 2 wt% Li_2CO_3.

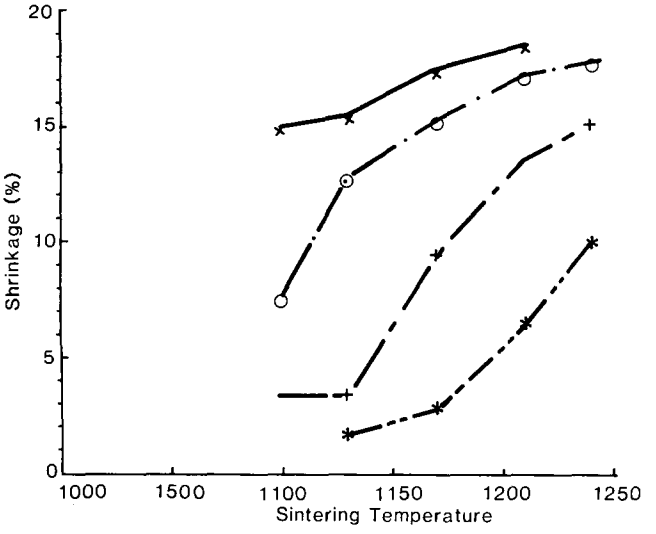

Fig. 4. Shrinkage of materials with 65 mol% KSN versus lithium carbonate amount and sintering temperature. – – – –, 0 wt% Li_2CO_3; – – –, 0·5 wt% Li_2CO_3; — · —, 1 wt% Li_2CO_3; ——, 2 wt% Li_2CO_3.

the behaviour of the different compositions are quite similar; the main differences due to both KSN and lithium carbonate are only temperature shifts. The shoulder between 500 and 600°C, unnoticeable on the curves corresponding to the bronze of the relaxors sintered with or without lithium, shows that the materials react together; the authors have not been able up to now to analyse this reaction more precisely.

3.2 X-Ray diffraction analysis

In every case the diffraction patterns of the mixed powders before sintering show together the two relaxors and the bronze when its concentration is greater than 5 mol%. After sintering, the two

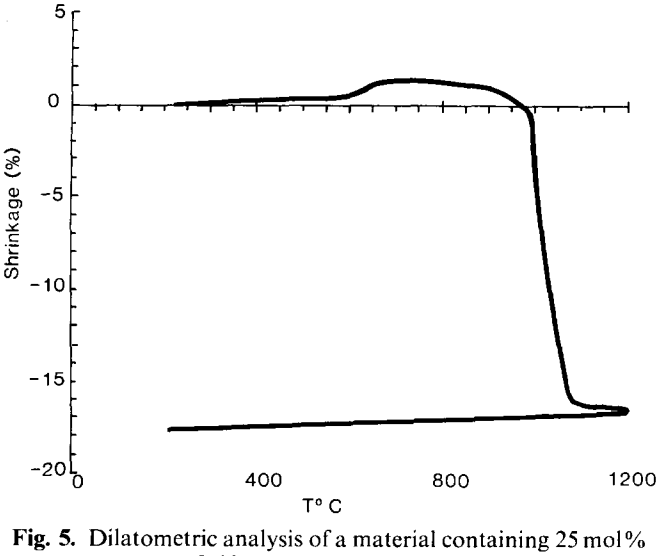

Fig. 5. Dilatometric analysis of a material containing 25 mol% KSN and 2 wt% Li_2CO_3.

Table 2. X-Ray diffraction analysis

Compositions with high concentrations of KSN (more than 25%)
The perovskite phases disappear between 1170 and 1210°C
The *c*/*a* ratio and the volume of the bronze cell are modified at 1100/1200°C
At the same time a new phase appears
Compositions with intermediate concentrations of KSN
The perovskite phases disappear near 1200°C
The *c*/*a* ratio and the volume of the bronze cell are modified at 1100/1200°C
At the same time a new phase appears
Presence of a pyrochlore phase up to 1130/1170°C
Compositions with low concentrations of KSN (≤5% KSN)
The perovskite phases do not disappear
The bronze phase is only noticeable after 1100°C, with a concentration depending on the sintering temperature
The *c*/*a* ratio and the volume of the bronze cell are modified at 1100/1130°C
At the same time a new phase appears
Presence of a pyrochlore phase at 1050°C which does not disappear at higher temperature

perovskites will have reacted and therefore will form a solid solution if always present.

Table 2 sums up the main results of the X-ray diffraction analysis performed on sintered ceramics, and Fig. 6 gives as examples the patterns corresponding to typical examples.

Three different behaviours can be described, depending on the initial bronze concentrations: low, i.e. less than 5 mol%; intermediate, i.e. 5–25 mol%; and high, i.e. greater than 25 mol%.

For intermediate and high KSN amounts, the perovskite phase disappears near 1200°C but remains in low KSN concentrations, only weaker. In this latter case, the bronze is not noticeable before sintering; it begins to be detected only at 1100°C. Also, in the case of low and intermediate KSN concentrations, the presence in large amounts of a pyrochlore phase that was not present in the starting materials can be seen. This pyrochlore phase disappears in the intermediate concentration case near 1100°C, while it remains in small amounts in the case of low KSN concentrations. It looks like the result of a reaction between the bronze and the

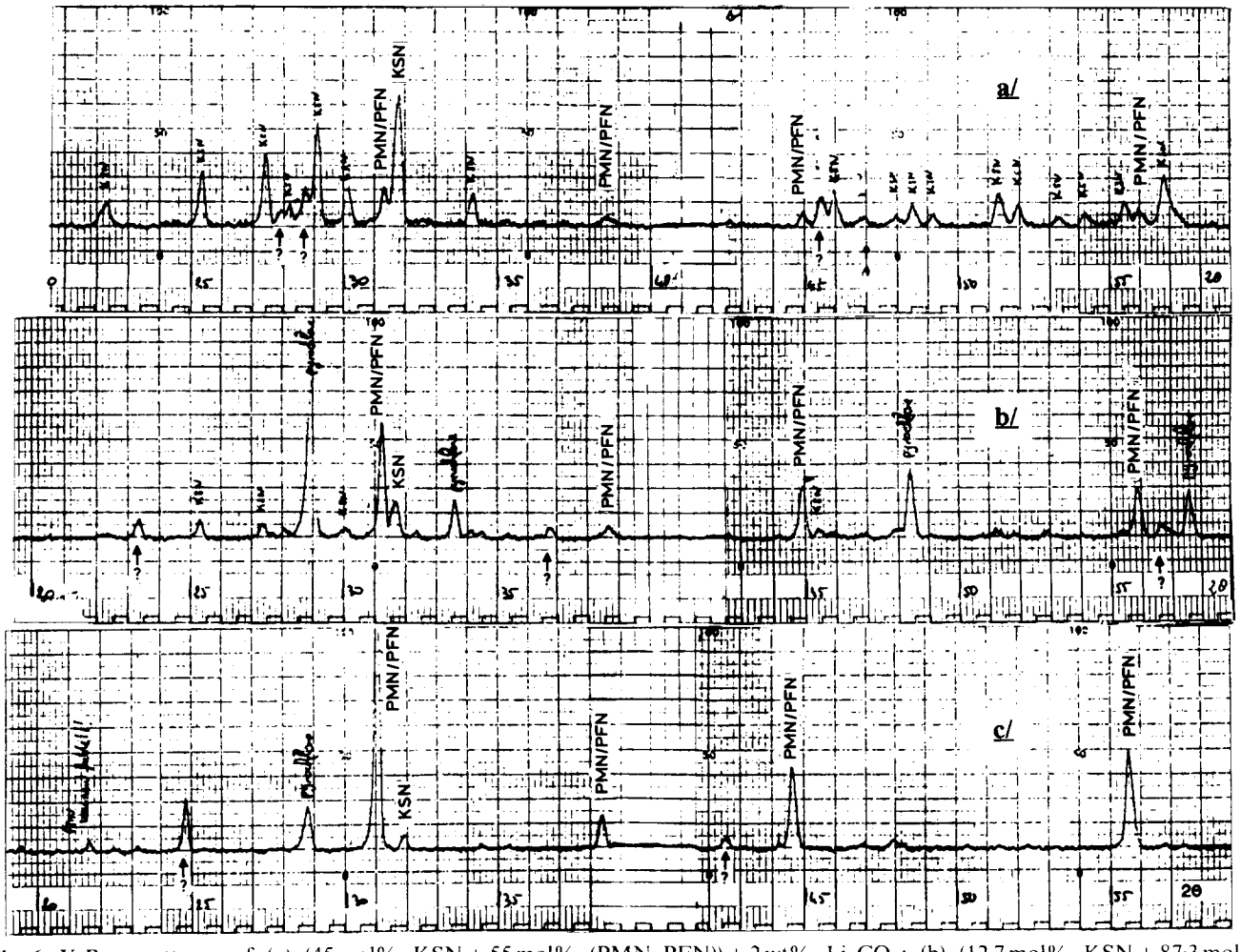

Fig. 6. X-Ray patterns of (a) (45 mol% KSN + 55 mol% (PMN–PFN)) + 2 wt% Li_2CO_3; (b) (12·7 mol% KSN + 87·3 mol% (PMN–PFN)) + 2 wt% Li_2CO_3; (c) (5 mol% KSN + 95 mol% (PMN–PFN)) + 2 wt% Li_2CO_3 sintered at 1110°C.

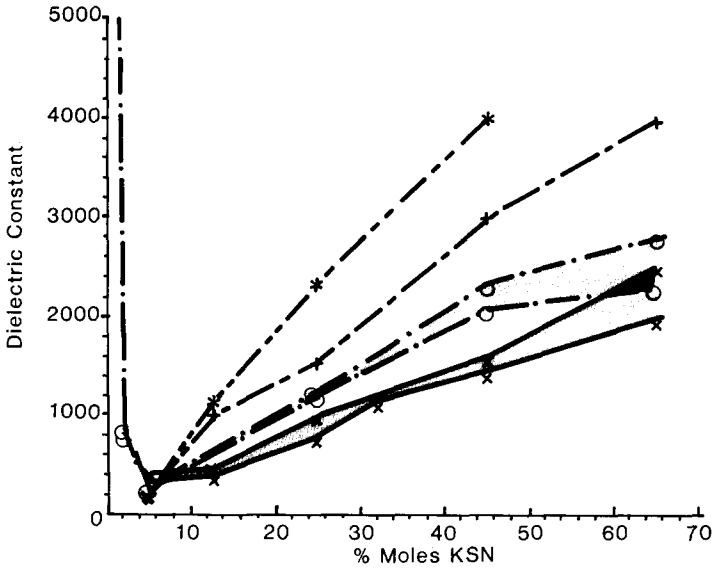

Fig. 7. Dielectric constant at room temperature versus KSN concentration and lithium carbonate amount. ——, 0 wt% Li_2CO_3; ——, 0·5 wt% Li_2CO_3; ——, 1 wt% Li_2CO_3; ——, 2 wt% Li_2CO_3.

perovskite, which disappears at higher temperature by reaction with the bronze when it is present in a sufficient amount.

This hypothesis is corroborated by the fact that the diffraction pattern of the bronze is transformed near 1100°C: in KSN, the c/a ratio of the elementary cell is close to $1\sqrt{10}$. This value varies slightly, as do the cell parameters, and as a consequence some diffraction peaks initially superimposed shift a little and are now distinct. Furthermore, the perovskite pattern is also modified, the parameter of the elementary perovskite cell decreasing when the KSN ratio increases. Correlatively, the presence of new peaks on the X-ray diffraction patterns are seen, pointing to the presence of a new phase that the authors have not been able to identify up to now.

It is important to note here that these evolutions exist either with or without the presence of lithium. Only the temperatures at which these phenomena occur differ: they are higher when there is no lithium. It seems that lithium, as was the case when it was used to sinter barium titanate or relaxors, helps the diffusion of the different elements. Similarly, it has been shown previously[14] that small lithium amounts could be introduced in perovskite phases, although they were hardly noticeable by X-ray diffraction analysis, leading then to new dielectric properties.

3.3 Dielectric properties

The dielectric properties of the sintered discs are quite different from those of either the pure KSN or of the relaxors, all these materials having a strong temperature dependence of the dielectric constant. On the contrary, the materials studied here have a slight temperature dependence of their dielectric constant, or can be characterized by a temperature coefficient of their dielectric constant.

Figure 7 shows that the values of the different dielectric constants at room temperature are strongly dependent on the KSN concentration, with a minimum close to 5 mol%. This figure includes the dielectric constant measured on densified ceramics versus the KSN concentration and the lithium carbonate amount.

It can be seen first that, at low KSN concentrations, the dielectric constant is very low, although the pure perovskite has a very high dielectric constant. This is certainly correlated to the strong reaction between the perovskite and the bronze, leading to a large concentration of pyrochlore phases. Such compositions are not of any interest.

On the other side of the graph, it is, on the contrary, very interesting to notice that the dielectric constant increases with the KSN concentration, and is, for a given composition, all the more important, since the lithium amount is low. The highest values are observed on discs sintered without any lithium.

Figure 8 shows a typical evolution of the dielectric constant temperature dependence versus the sintering temperature. In every case the curves $\varepsilon = f(T)$ have a decreasing slope at low temperatures, below room temperature, and may either decrease again at higher temperatures or increase toward higher values. For a given composition, this behaviour seems to depend both on lithium amount and on sintering temperature. These phenomena seem

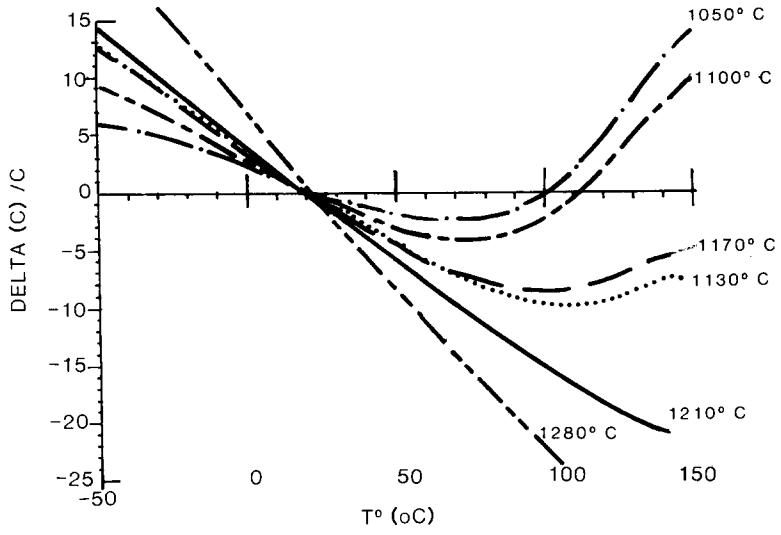

Fig. 8. Dielectric constant temperature dependence versus the sintering temperature of the material with 45 mol% KSN and 2 wt% Li_2CO_3.

sometimes to be correlated with the crystallographic evolution. It seems that the ceramic is formed of a mixture of the distorted bronze having a low Curie temperature, and of the initial bronze that has a high Curie temperature. There is no more perovskite phase present in the sintered ceramics. The higher the sintering temperature, the more the ceramic homogenizes in the distorted bronze, leading then to a linear temperature-dependent characteristic.

These characteristics are obtained when, for every KSN concentration, the sintering temperature is high enough to make the dielectric characteristic decrease in the high-temperature range. In these cases, curves are obtained that are very surprisingly not far from straight lines, as shown in Fig. 9. The authors wonder what this particular behaviour

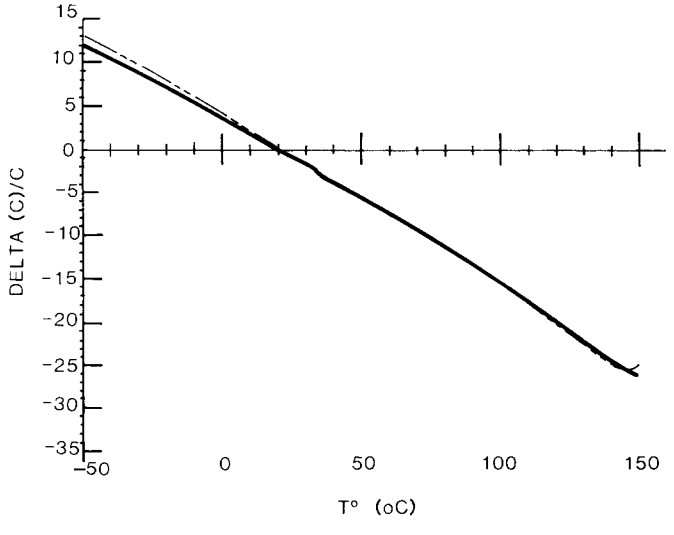

Fig. 9. Linear temperature dependence of the dielectric constant of materials with 45 mol% KSN and 2 wt% Li_2CO_3: ——, sintered at 1210°C; — — —, sintered at 1240°C.

means, as X-ray diffraction patterns are very difficult to analyse, and as the precise structure evolution is not exactly understood.

There is a most important observation to point out concerning the lithium behaviour: linear characteristics were never obtained either without any lithium or with too high lithium amounts. This is illustrated in Fig. 10, where the characteristics of the ceramics with 65 mol% KSN are gathered; it is only with the 1 wt% lithium carbonate concentration that it is possible to get this behaviour with a sintering temperature of 1240°C. For the 45 mol% KSN compositions, only 1 and 2 wt% lithium carbonate lead to real linear materials. This is also observed for intermediate KSN concentration materials. It is only with low KSN concentrations that 0·5 wt% of lithium carbonate additions allow such characteristics to be obtained, but, once again, some lithium is always necessary.

This particular behaviour has certainly to be correlated to the hypothesis of the introduction of lithium in the lattice, but only lithium concentration measurements in ceramics correlated, for example with the values of the temperature coefficient, can help to obtain an unambiguous answer to that question.

3.4 Electrical properties

Table 3 shows the evolution of the resistivity of materials sintered at different temperatures, with two different lithium additions. These measurements were made with a DC bias of 100 V/mm.

It can be easily seen that, for each KSN concentration, the resistivity increases with the sintering temperature, and then decreases if the

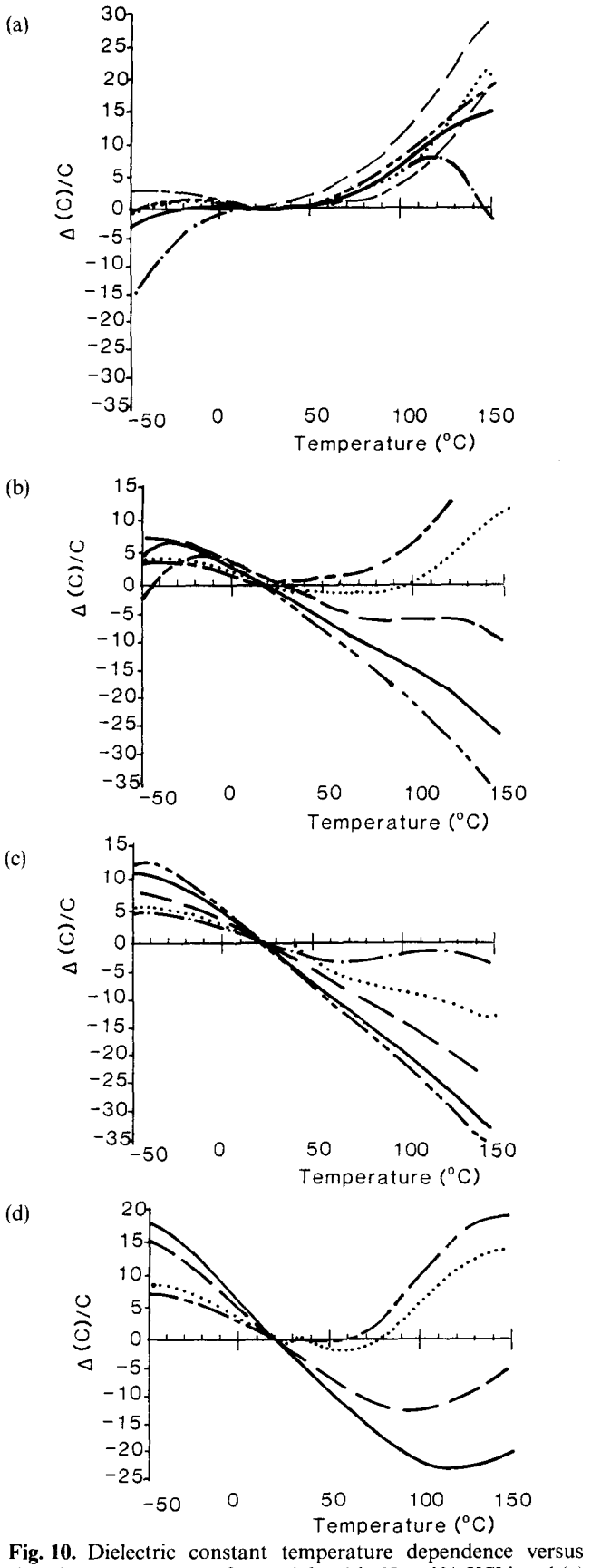

Fig. 10. Dielectric constant temperature dependence versus sintering temperature of materials with 65 mol% KSN and (a) 0 wt% Li_2CO_3; (b) 0·5 wt% Li_2CO_3; (c) 1 wt% Li_2CO_3; (d) 2 wt% Li_2CO_3. Sintering temperature: ——, 1100°C; ·····, 1130°C; – –, 1170°C; ———, 1210°C; — – —, 1240°C; — · —, 1255°C.

sintering temperature is too high. When the insulation resistance is good, increasing the DC bias up to 1500 V/mm does not lead to any significant evolution.

For every sintering temperature, only some bronze concentrations lead to good values. In fact, a 'cloud' including the compositions and their sintering temperatures can be drawn on each chart, including those that lead to quite good values of resistivity.

The resistivity is never high when there is no lithium introduction. So, for each composition, there seems to be a compromise between parameters such as the amount of lithium remaining in the ceramic after sintering, the amounts of volatile elements (mainly lead) and the exact crystallographic composition, which lead to a consequent defect chemistry taking, therefore, the sintering temperature into account.

3.5 Losses

The losses at room temperature are generally good, and every time the resistivity is high, i.e. higher than 10^6 Mol. cm, they remain low when the temperature increases. Their value is then not far from 0·5 mol%. In fact, the characterization of the material has been made on discs metallized with an In–Ga alloy, which cannot lead to better values. So, although the authors are not able to assert unambiguously that these ceramics have all the specifications of the EIA standards, they are certainly not far from type I materials.

4 Stable Type II Ceramics

Section 3 concerns the perovskite side of the relaxor/TTB diagram. In contrast, compositions corresponding to the bronze side of the diagram can lead to type II stable dielectric materials (see Appendix). Moreover, to get high dielectric constants ceramics with the X7R specification, amounts of various perovskites with various Curie temperatures are also added to these materials.

4.1 Pure bronze ceramics

The sintering of KSN in the presence of a lithium salt has already been studied.[15] The calcined oxide added with 2 wt% $LiNO_3$ or 1·2 wt% Li_2CO_3 can be sintered at 1200°C, with a good densification, in contrast to pure KSN. The curves $\varepsilon = f(T)$ (Fig. 11) show the effect of the lithium salts addition upon the dielectric characteristics.

For example, with $LiNO_3$, a maximum displaced

Table 3(a). Resistivity (MΩ cm) of materials sintered with 0·5 wt% Li_2CO_3

KSN (%)	*1240°C*	*1210°C*	*1170°C*	*1130°C*	*1100°C*	*1050°C*
65	$6{\cdot}5 \times 10^2$	$6{\cdot}5 \times 10^3$	$2{\cdot}4 \times 10^3$	$2{\cdot}5 \times 10^2$	$1{\cdot}1 \times 10^3$	—
45	$2{\cdot}4 \times 10^4$	$9{\cdot}5 \times 10^5$	$2{\cdot}9 \times 10^4$	$3{\cdot}8 \times 10^2$	$4{\cdot}4 \times 10^2$	—
25	2×10^6	$2{\cdot}7 \times 10^7$	$5{\cdot}5 \times 10^6$	6×10^2	$5{\cdot}5 \times 10^2$	—
13	3×10^4	1×10^8	1×10^8	7×10^2	$1{\cdot}1 \times 10^3$	3×10^2
5	$3{\cdot}2 \times 10^3$	1×10^8	$4{\cdot}2 \times 10^6$	1×10^3	$1{\cdot}5 \times 10^2$	—

Table 3(b). Resistivity (MΩ cm) of materials sintered with 2 wt% Li_2CO_3

KSN (%)	*1280°C*	*1210°C*	*1170°C*	*1130°C*	*1100°C*	*1050°C*
65	—	2×10^4	6×10^3	1×10^3	2×10^3	—
45	5×10^6	1×10^8	8×10^5	2×10^4	6×10^3	$3{\cdot}3 \times 10^3$
32	—	$4{\cdot}4 \times 10^6$	$5{\cdot}7 \times 10^7$	$1{\cdot}3 \times 10^5$	4×10^5	$1{\cdot}3 \times 10^4$
25	—	6×10^5	1×10^6	4×10^5	5×10^4	$3{\cdot}4 \times 10^5$
13	—	8×10^2	2×10^3	$1{\cdot}5 \times 10^3$	3×10^5	$7{\cdot}5 \times 10^3$
5	—	5×10^1	2×10^2	3×10^1	5×10^6	$3{\cdot}5 \times 10^2$

towards lower temperatures is observed, i.e. at about 125°C instead of 180°C for KSN sintered without lithium, with a promising dielectric constant of about 4000, close to this diffuse maximum. A similar effect is observed with lithium carbonate, but with a smaller shifting of the maximum of ε (145°C). The modifications of the $\varepsilon = f(T)$ curves strongly suggest that lithium has entered into the TTB lattice either on the octahedral sites or on the prismatic trigonal sites. The good resistivities (see Table 4) observed agree with this hypothesis. However, the corresponding X-ray diffraction patterns show only very slight modifications. This is not surprising, as Pouchard *et al.*[16] noted that, in TTB structures, the *c/a* ratio could not easily be correlated with the Curie temperature. Furthermore, higher sintering temperatures lead to a gathering of the Curie temperatures in all lithium additions at a temperature close to 120°C in the case of 1250°C, 110°C in the case of 1300°C, and increases again to 120°C when sintering occurs at 1350°C. This behaviour can be explained as if, when the sintering temperature increases, lithium may enter equally in each case into the lattice, but evaporates when the temperature is high enough. However, the corresponding X-ray patterns (see Fig. 12) point out that the *c/a* ratio decreases significantly, but with a behaviour depending on the nature of the lithium salt. Once more, the *c/a* ratio cannot be correlated to the Curie temperature. In respect of this, action of lithium carbonate and nitrate on this structure exhibits some similarity with the case of different perovskites.[14] This is not surprising, since the TTB structure (Fig. 1) is built up from perovskite blocks (Fig. 2); only the way of linking the oxygen octahedra are different in both structures.

Table 4. Resistivities of stable type II ceramics measured under 60 V DC

Nominal composition	*Lithium salt (wt%)*	*Sintering schedule (°C, h)*	*ρ (Ω cm)*
KSN	Li_2CO_3, 1·2	1200, 2	7×10^{10}
	$LiNO_3$, 2	1200, 2	8×10^{11}
5 KSN + 0·5 PMN	Li_2CO_3, 1·2	1200, 2	10^{13}
	Li_2CO_3, 2	1200, 2	$3{\cdot}5 \times 10^{11}$
	$LiNO_3$, 2	1200, 2	2×10^{12}
5 KSN + 0·5(0·77 PMN + 0·23 PFN)	Li_2CO_3, 1·2	1200, 2	3×10^{11}
4·5 KSN + 0·55 PFT	Li_2CO_3, 0·25	1250, 1	$1{\cdot}5 \times 10^{12}$
		1300, 4	$2{\cdot}5 \times 10^{12}$
4·5 KSN + 0·55 PMT	LiF, 0·25	1250, 3	3×10^8
		1300, 2	5×10^{12}
4·5 KSN + 0·5 PFT + 0·04 $BaTiO_3$	$BaLiF_3$, 0·01 (mol%)	1250, 2	2×10^8
		1300, 2	10^{11}

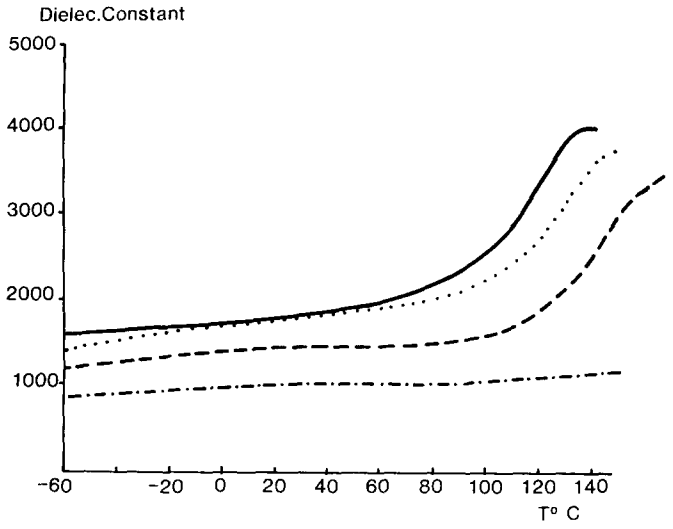

Fig. 11. Relative permittivity ε versus temperature for – – –, pure KSN sintered at 1300°C, 2 h; — · —, KSN + 2 wt% LiF sintered at 1200°C, 2 h; ——, KSN + 2 wt% $LiNO_3$ sintered at 1200°C, 2 h; · · · · ·, KSN + 1·2 wt% Li_2CO_3 sintered at 1200°C, 2 h.

The role of the lithium salt is visible on the microstructures (Fig. 13) corresponding to thermally etched samples. Pure KSN sintered at 1350°C, 2 h has a residual porosity (Fig. 13(a)) that practically disappears when sintered at 1200°C in the presence of 1·2 wt% Li_2CO_3 (Fig. 13(b)). One observes in the latter case larger grains ($\approx 10\,\mu m$) surrounded by small ones.

4.2 TTB bronzes with PMN perovskite ceramics

Attempts have been made to improve the dielectric properties of well densified KSN by introducing small amounts of perovskites owing to their high dielectric constant and to their low Curie temperature. The aim is to synthesize a ceramic formed of mixed phases from the solid-state reactions occurring during the co-sintering of the KSN and perovskites phases.

The first choice was the ferroelectric perovskite $Pb(Mg_{1/3}Nb_{2/3})O_3$ (PMN), which exhibits a high dielectric constant of 12 000 at the Curie temperature ($T_C \approx -12°C$). Different mixtures xKSN + yPMN were thus sintered in the presence of 1·2 wt% Li_2CO_3 at 1200°C, 2 h. The curves $\varepsilon = f(T)$ (Fig. 14) show that the addition of a small amount of PMN (i.e. less than 10 mol%) leads to a spectacular modification of these curves. The maxima of the curves can be displaced from 125°C towards −20°C. These broad maxima are characterized by quite high dielectric constants (higher than 2500) and which

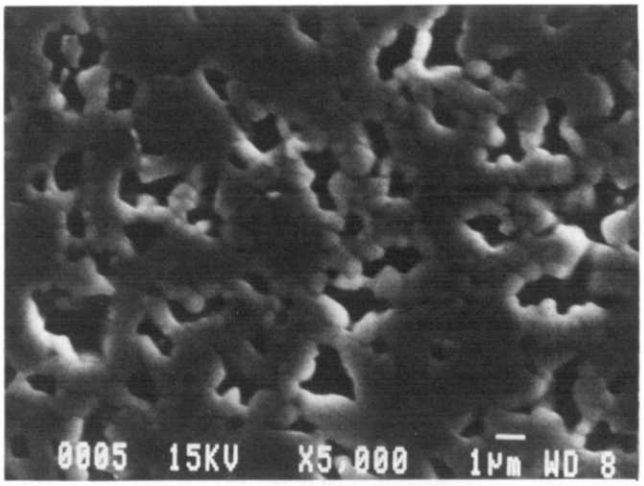

(a)

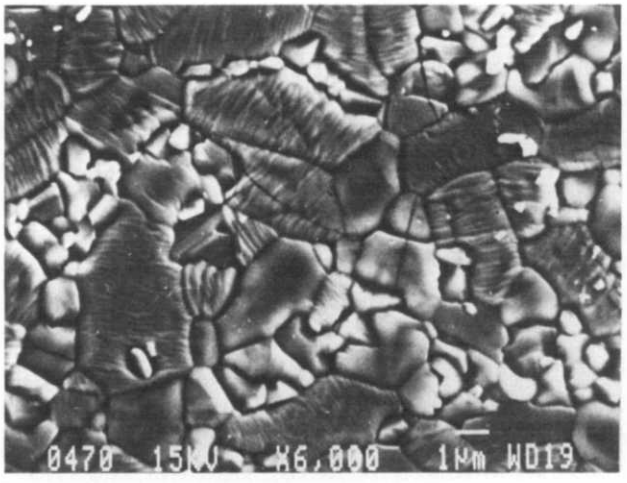

(b)

Fig. 13. Microstructures of thermally etched samples: (a) pure KSN sintered at 1300°C, 2 h and (b) KSN + 1·2 wt% Li_2CO_3 sintered at 1200°C, 2 h.

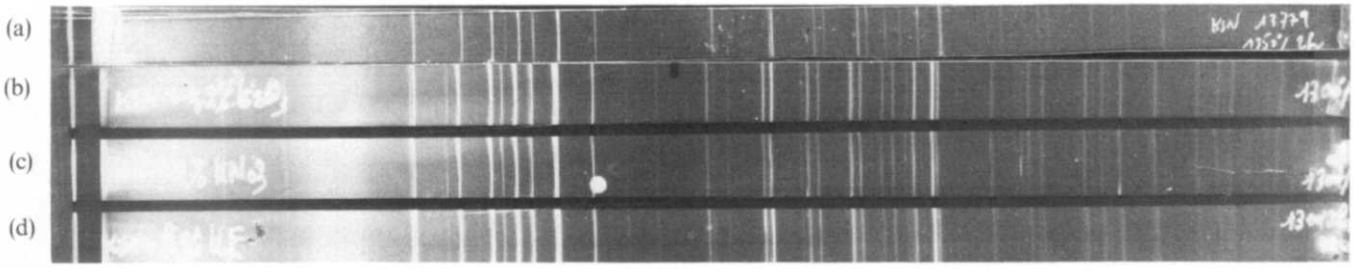

Fig. 12. X-Ray patterns of ceramics sintered at 1300°C, 2 h: (a) pure KSN; (b) KSN + 1 wt% Li_2CO_3; (c) KSN + 2 wt% $LiNO_3$; (d) KSN + 2 wt% LiF.

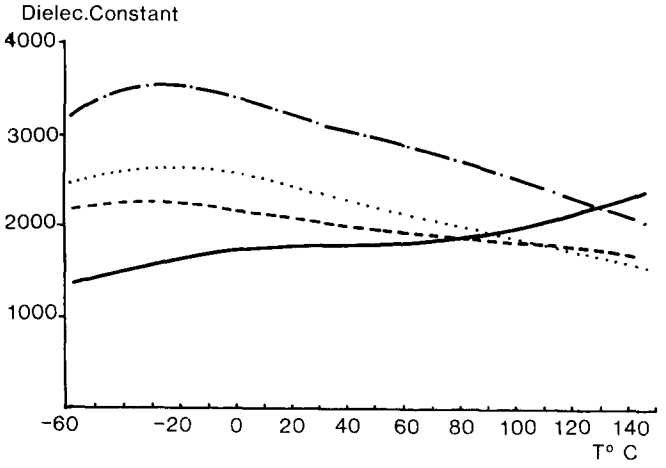

Fig. 14. Relative permittivity ε versus temperature for compositions xKSN + yPMN sintered at 1200°C in the presence of 1·2 wt% Li_2CO_3 using different soak times: ——, 5 KSN + 0·5 PMN, 1200°C, 1 h; – – –, 5 KSN + 0·5 PMN, 1200°C, 2 h; — · —, 5 KSN + 0·7 PMN, 1200°C, 4 h; · · · · ·, 3 KSN + 0·7 PMN, 1200°C, 2 h.

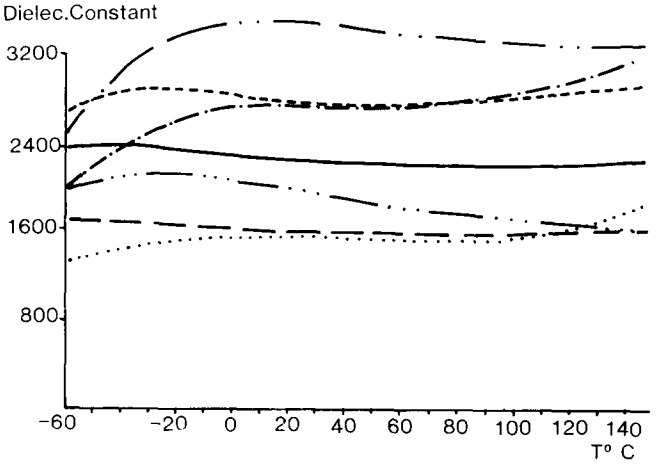

Fig. 15. Relative permittivity ε versus temperature for the KSN–PMN system; influence of the composition, of the nature of the lithium salt and of the sintering temperature: — —, 3 KSN + 0·7 PMN + 1 wt% LiF sintered at 1200°C, 2 h; – – –, 3·5 KSN + 0·65 PMN + 1 wt% LiF sintered at 1200°C, 1 h; — · —, 3·5 KSN + 0·65 PMN + 1 wt% LiF sintered at 1225°C, 1 h; ——, 4 KSN + 0·6 PMN + 1 wt% LiF sintered at 1200°C, 1 h; — · —, 4·5 KSN + 0·55 PMN + 1 wt% LiF sintered at 1200°C, 1 h; · · · · —, 5 KSN + 0·5 PMN + 1 wt% Li_2CO_3 sintered at 1200°C, 1 h; · · · · ·, 5 KSN + 0·5 PMN + 2 wt% $LiNO_3$ sintered at 1200°C, 1 h.

can reach 3500, associated with high resistivities (see Table 4). Figure 14 points out, moreover, the influence of the thermal cycle. It can be seen that for short dwelling times almost linear curves $\varepsilon = f(T)$ are obtained with a positive slope. In contrast, an increase of the dwelling time favours the formation of a low-temperature maximum.

A second important point deals with the influence of the nature of the lithium salt upon the dielectric characteristics. Contrary to the case of pure KSN, the dielectric constant is significantly increased whatever the nature of the lithium salt is. Flat curves are thus obtained with LiF (Fig. 15) for compositions close to 4 KSN + 0·6 PMN, with much higher dielectric constants than for pure KSN sintered in the presence of LiF. Moreover, the presence of two flat maxima respectively close to −30 and 150°C suggest the presence of inhomogeneous phases. Nevertheless, the ε values not higher than 3000 remain too low in each case for industrial applications. However, the thermal cycle is so far not optimized and an increase of the sintering temperature can lead to ε values greater than 3000, but at the expense of the flatness of the curve $\varepsilon = f(T)$ (see Fig. 15, the curve for 1225°C).

In the case of LiF, the X-ray diffraction patterns did not allow a mixture of two phases to be detected, but only a TTB phase to be identified (see Fig. 16). Moreover, large cell parameters modifications (c/a and the volume cell decrease) were observed, in agreement with a reaction occurring during sintering between the perovskite, the lithium fluoride and the bronze, as was the case in the behaviours presented in Section 3.2. Nevertheless, the presence of small amounts of perovskite phase besides the TTB cannot be ruled out, especially if one bears in mind that the TTB exhibits a '$a/\sqrt{10}$' parameter close to the a parameter of the perovskite.

In the case of lithium carbonate, the perovskite disappears only when sintering at 1250°C. The X-ray diffraction pattern shows that the bronze structure is this time mainly transformed only by the c/a ratio

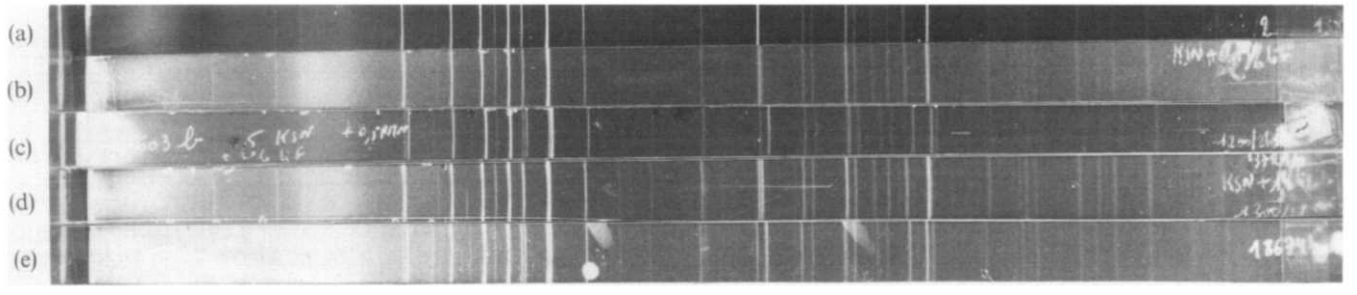

Fig. 16. X-Ray diffraction patterns of sintered KSN + PMN + lithium salts compositions: (a) pure KSN (1200°C, 2 h); (b) KSN + 2 wt% LiF (1300°C, 2 h); (c) 5 KSN + 0·5 PMN + 2 wt% LiF (1200°C, 2 h); (d) KSN + 1 wt% Li_2CO_3 (1300°C, 2 h); (e) 3·5 KSN + 0·65 PMN + 1 wt% Li_2CO_3 (1250°C, 2 h).

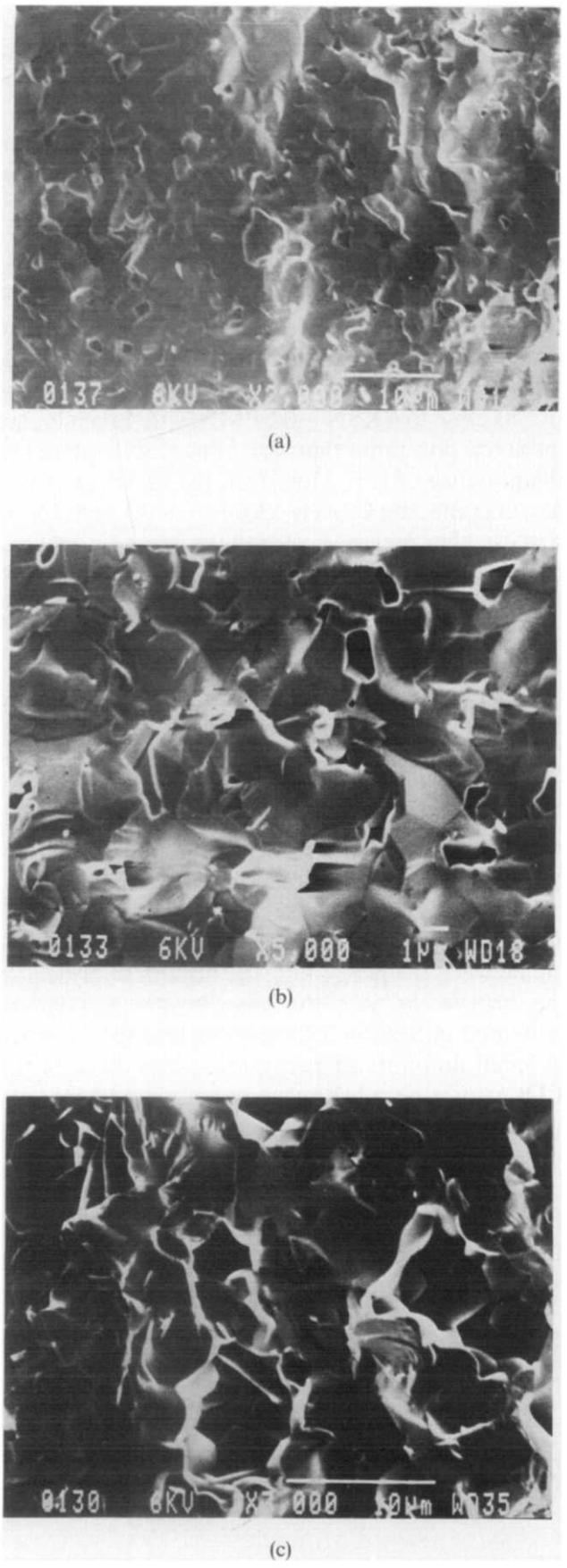

Fig. 17. Evolution of the microstructure (fractures) versus temperature for 4·5 KSN + 0·55 PMN + 1 wt% Li_2CO_3: (a) 1150°C, 1 h; (b) 1200°C, 1 h; (c) 1250°C, 1 h.

modification (see Fig. 16). In previous studies,[14] the particular behaviour observed was demonstrated when either lithium alone or lithium and fluorine are introduced into the barium titanate lattice, leading in the case of lithium and fluorine to large modifications of the c/a ratio and of the volume of the cell, and a correlated flatness of the $\varepsilon = f(T)$ characteristic. All that is presented here may be interpreted in a similar manner.

The microstructures observed for composition 4·5 KSN + 0·55 PMN + Li_2CO_3 sintered at different temperatures (Fig. 17) do not allow a second phase to be detected on fractured samples. It can also be seen on Fig. 17 that the densification and the microstructure are closely related to the sintering temperature.

Comparison between Fig. 13 and Fig. 17 shows that the addition of lead perovskites to KSN does not delay the densification and leads to a more homogeneous microstructure. The shape of the grains is more regular and the largest grains are not bigger than 5–6 μm.

4.3 Bronzes with other relaxor materials

4.3.1 KSN + (PMN–PM′N), M′ = Fe, Zn

The decrease of the dielectric constant at low temperature (Fig. 15) suggests that the perovskite PMN could be advantageously replaced by a perovskite solid solution 0·77 PMN + 0·23 PM′N (M′ = Fe or Zn), which has a very high dielectric constant ($\varepsilon \approx 35\,000$) and a T_C close to 25°C.[12,13] Figure 18 shows once more that it is possible to

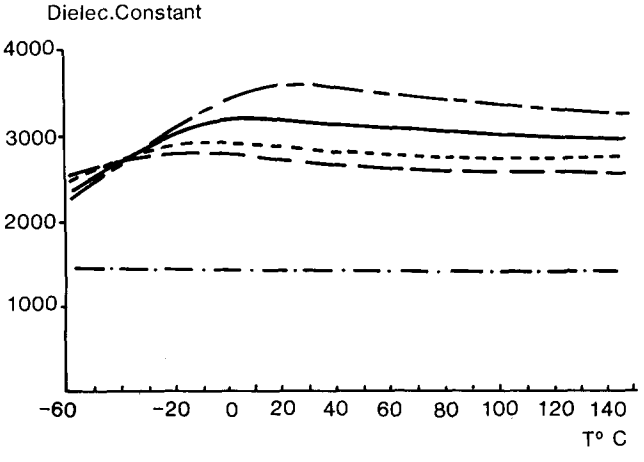

Fig. 18. Relative permittivity ε versus temperature for the KSN–(PMN–PFN) system sintered in the presence of different lithium salts with different sintering schedules: ——, 4·5 KSN + 0·55(0·77 PMN + 0·23 PFN) + 1 wt% Li_2CO_3 sintered at 1250°C, 1 h; – – –, 4·5 KSN + 0·55(0·77 PMN + 0·23 PFN) + 1 wt% Li_2CO_3 sintered at 1200°C, 1 h; ——, 4·5 KSN + 0·55 (0·77 PMN + 0·23 PFN) + 1 wt% Li_2CO_3 sintered at 1150°C, 1 h; — — —, 4·5 KSN + 0·55(0·77 PMN + 0·23 PFN) + 2 wt% Li_2CO_3 sintered at 1150°C, 1 h; — · —, 4·5 KSN + 0·55 (0·77 PMN + 0·23 PFN) + 2 wt% LiF sintered at 1250°C, 1 h.

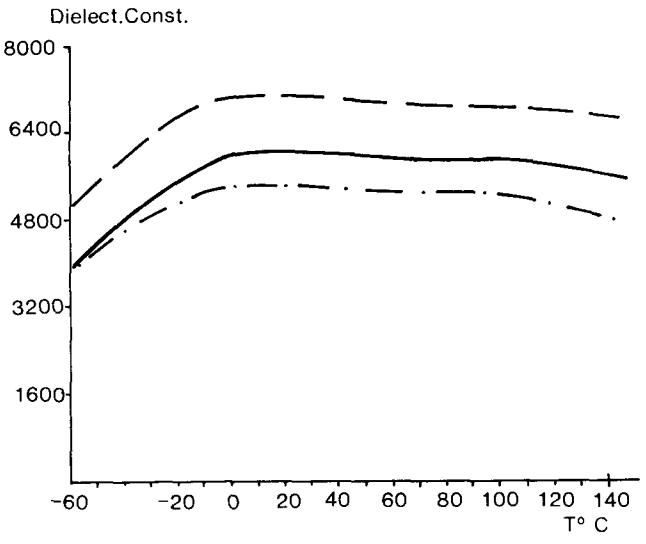

Fig. 19. Relative permittivity ε versus temperature for the systems KSN–PMT and KSN–PFT: —·—, 4·5 KSN + 0·55 PMT + 0·25 wt% LiF sintered at 1300°C, 2 h; — —, 4·5 KSN + 0·55 PMT + 0·25 wt% LiF sintered at 1225°C, 3 h; ——, 4·5 KSN + 0·55 PFT + 0·25 wt% Li_2CO_3 sintered at 1300°C, 2 h.

obtain with these new systems materials with a dielectric constant higher than 3500, but without a flat profile and having resistivities higher than 10^{11} Ω cm. In fact, curves are flat above room temperature but the dielectric constant decreases generally drastically at low temperature, and one observes a broad maximum around 0–20°C. These results confirm that the shape of the curve $\varepsilon = f(T)$ is closely related to the composition, and that for a given composition it depends on the sintering schedule.

The corresponding decrease of the average level of the dielectric constant above room temperature when the sintering temperature increases (Fig. 18) is quite unusual but can be explained by an increase of ε at low temperature due to a modification of the composition of the solid solution (better homogenization).

4.3.2 KSN + PMT (M = Mg, Fe)

The above results (Section 4.3.1) correspond to flat curves, except for temperatures below room temperature. They have been obtained by mixing a TTB having a $T_C \approx 150$°C with a perovskite having a T_C close to room temperature. Best results may be obtained by using a perovskite having a low Curie temperature. So lead tantalate perovskites Pb-$(Ta_{1/2}Fe_{1/2})O_3$ (PFT) and $Pb(Mg_{1/3}Ta_{2/3})O_3$ (PMT), which exhibit low Curie temperatures, respectively −40 and −100°C, have been substituted for lead niobate perovskites to increase the dielectric constant below room temperature.

Unfortunately, this leads to the same drastic decrease of ε at low temperature (Fig. 19) as with lead niobate. The general shape of the curve $\varepsilon = f(T)$, characteristic of a ceramic made of mixed phases, seems to be independent of the Curie temperature of the perovskite. That could be interpreted as if the initial perovskite structure disappears, leading to phases derived from the TTB KSN. This is confirmed by the X-ray diffraction patterns (see Fig. 20), pointing out that, whatever the sintering temperature and the nature of the perovskite and of the lithium salt, no perovskite phase can be detected. Furthermore, the c/a ratio of the TTB decreases but, this time, no variation of the volume cell can be observed whatever the nature of the lithium salt. However, this study is not completely negative, since it was found that dielectric constants close to 6000 can be obtained when substituting Nb by Ta. If one considers that both structures are quite equivalent, the difference can be attributed to the relative polarizability of Nb and Ta.

4.4 Bronzes with other perovskite ceramics

The above results (Section 4.3) show that the authors have not been able to synthesize, by mixing KSN with only one relaxor perovskite, dielectric ceramics leading simultaneously to the X7R specifications and to high dielectric constants.

This can be due to the fact that it is difficult to obtain an inhomogeneous solid solution because of the high sintering temperature; by adding a lithium salt as a sintering agent, this sintering temperature

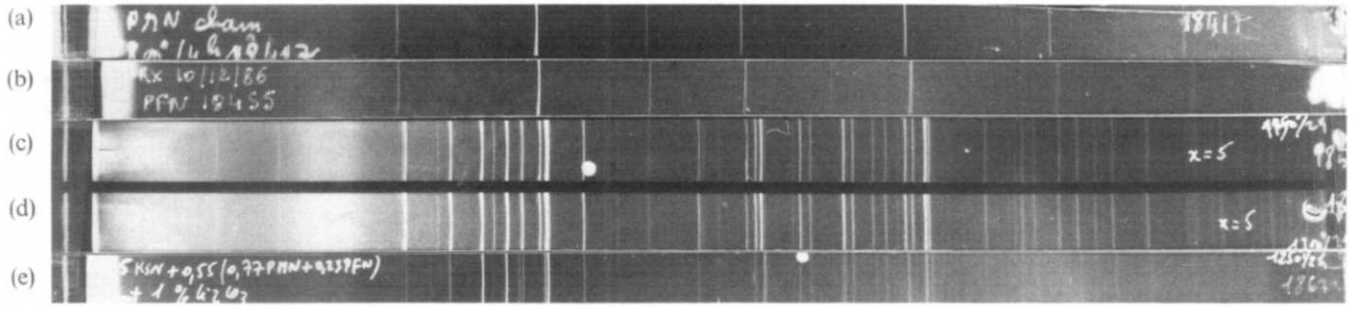

Fig. 20. X-Ray pattern of sintered KSN + (PMN–PFN) + 1 wt% Li_2CO_3 compositions: (a) pure PMN; (b) pure PFN; (c) composition sintered at 1150°C, 2 h; (d) composition sintered at 1200°C, 2 h; (e) composition sintered at 1250°C, 2 h.

can be decreased but at the same time the diffusion phenomena are enhanced; the aspect of the curves $\varepsilon = f(T)$ shows that the positive influence of the perovskite, which is supposed to increase the dielectric constant below room temperature is lost.

It is well known that a random distribution of different species on a given crystallographic site always leads to a diffuse ferroelectric–paraelectric transition.[17] Thus, several attempts have been made in order to prepare a complex composition, corresponding to several cations introduced either in the tunnels or in the octahedral sites of the TTB structure.

Compositions described in Section 4.3.1 introduce large cations K, Sr and Pb into the pentagonal and square tunnels but only niobium (or tantalum) and magnesium into the octahedral sites of the TTB structures. An attempt was made to introduce simultaneously tantalum and titanium into these octahedral sites besides niobium and iron.

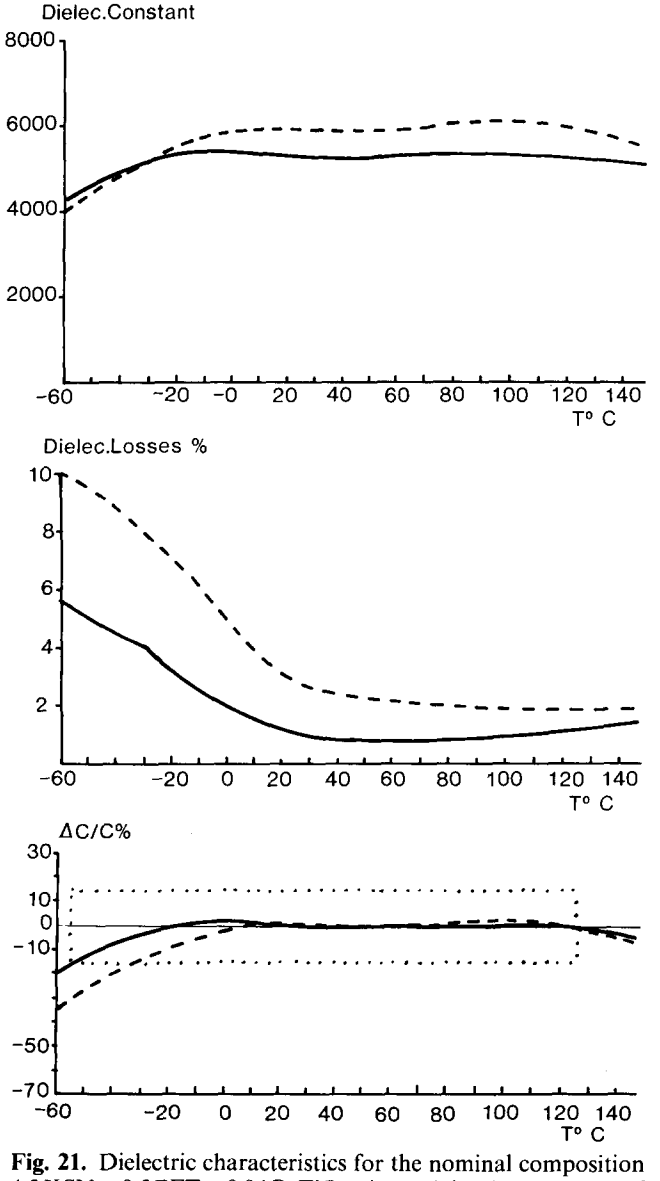

Fig. 21. Dielectric characteristics for the nominal composition 4·5 KSN + 0·5 PFT + 0·04 $BaTiO_3$ sintered in the presence of 0·01 $BaLiF_3$ as sintering agent: – – –, 1250°C, 1 h and ——, 1300°C, 1 h.

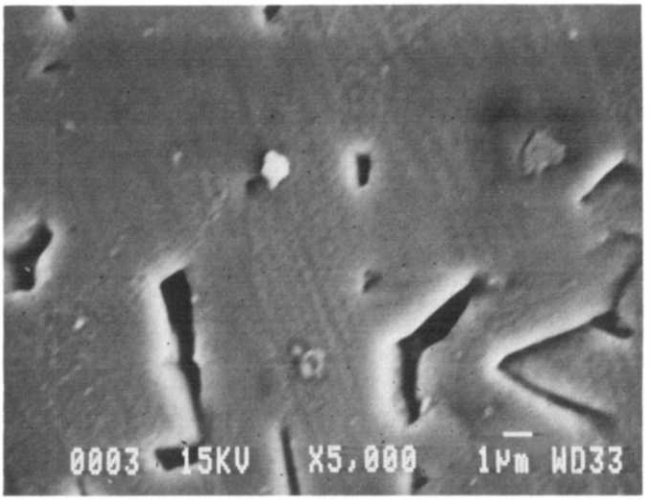

Fig. 22. Microstructure of the composition of Fig. 21 sintered at 1250°C, 1 h.

Titanium was introduced in the form of $BaTiO_3$, owing to the ability of this perovskite to exhibit flat curves for capacitors. Small amounts of presintered $BaTiO_3$ were added to the composition 4·5 KSN + 0·5 PFT, which exhibits high dielectric constants. $BaLiF_3$ was added as a sintering agent.[18]

Figure 21 shows the results corresponding to composition 4·5 KSN + 0·5 PFT + 0·04 $BaTiO_3$ + 0·01 $BaLiF_3$ sintered at 1250 or 1300°C, 1 h.

As for pure perovskites, $BaLiF_3$ acts as a sintering agent. A quite good densification (Fig. 22) is obtained as soon as 1250°C is reached, in spite of the refractory character of tantalum. However, the shape of the curve $\varepsilon = f(T)$ is then practically identical to the case of 4·5 KSN + 0·5 PFT sintered in the presence of LiF or Li_2CO_3, and the corresponding dielectric losses are high (Fig. 21(b)), while the resistivities are relatively low, i.e. $10^8\ \Omega$ cm (see Table 4). On the contrary, by sintering this complex composition at 1300°C, 1 h, a slight decrease of the mean level of the dielectric constant is observed associated with a flat profile of the curve with a decrease of the dielectric losses and a large increase of the resistivities (see Table 4). A flat curve $\varepsilon = f(T)$ with an average value of 5500, practically compatible with the X7R specification, is obtained.

5 Concluding Remarks

The dielectric ceramics presented in the first part of this paper associate relaxor materials with a

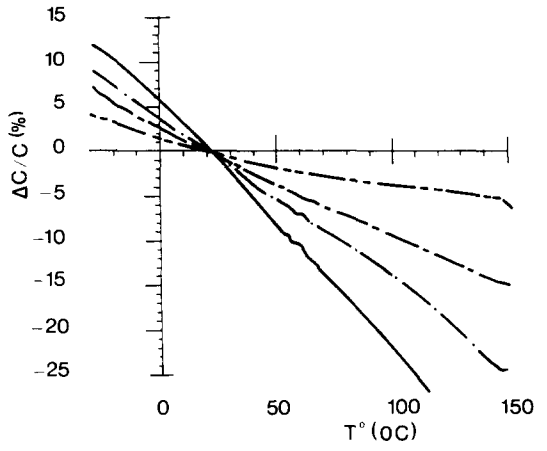

Fig. 23. Dielectric constant temperature dependence of some different materials.

tetragonal tungsten bronze in the perovskite side of the diagram. Lithium carbonate additions were used to promote densification and to obtain specific electric and dielectric characteristics. After sintering these materials at different temperatures, it was observed that, in addition to stable type II materials, these compositions can lead to type I materials with a negative temperature coefficient. Figure 23 gathers some typical dielectric constant temperature dependence corresponding to materials with high resistivities.

During the sintering cycle, the diffraction pattern of the bronze is transformed near 1100°C. Correlatively, the presence of new peaks was noted on the X-ray diffraction patterns, pointing out the presence of a new phase. It looks as if this new phase has a low Curie temperature, and is mixed with the modified and distorted bronze phase that has a high temperature Curie point. There is no more perovskite phase present in the high-temperature sintered ceramics. The higher the sintering temperature, the more the ceramic homogenizes in the distorted bronze, and then has a linear dielectric constant temperature dependence.

Type I characteristics were never obtained either without lithium or with too high lithium amounts. On the other hand, the resistivity is never high when there is no lithium introduction. Thus, for each composition, there seems to exist a compromise between the different parameters. The lithium remaining in the ceramic after sintering, the amounts of volatile elements (mainly lead) and the exact crystallographic composition lead to a consequent defect chemistry, taking, therefore, the sintering temperature into account. But only lithium concentration measurements in ceramics correlated, for example with the values of the temperature coefficient, with the resistivity and with the evolution of the X-ray diffraction patterns, could help the understanding of these particular behaviours. Up to now the authors have never been able to correlate the slope of the dielectric characteristic versus temperature, either with the dielectric constant or with any other parameter such as the composition. However, reproducible ceramics are obtained, but the authors are not able to explain and predict all their properties.

The second part of this paper, which deals with the TTB-rich mixtures, shows a very different behaviour. One observes that high dielectric constants (higher than 6000) can be obtained compatible with the X7R specification and accompanied by low dielectric losses. Resistivities measured with a 60-V DC bias are quite correct, generally close to 10^{11} or 10^{12} Ω cm. These good values are obtained in spite of the use of a lithium salt as a sintering agent, and can be explained by a quasi-total evaporation of the lithium salt during sintering, as confirmed by chemical analysis. The X-ray diffraction patterns show large modifications of the cell parameters of the TTB, pointing out the introduction of lithium in the structure, and the formation of TTB-type solid solution between the bronze and the perovskites. These modifications lead to an increase of the c/a ratio without any evident correlation with the evolution of the dielectric properties.

The consideration of the microstructures associated with the dielectric characteristics show that the use of a niobate with a TTB structure associated with some perovskites can be used for the elaboration of type II multilayer ceramic capacitors having high dielectric constants close to 6000 and flat curves.

References

1. Shrout, T. R. & Dougherty, J. P., A world view on lead based $Pb(B_1B_2)O_3$ relaxors vs $BaTiO_3$ based dielectric for multilayer capacitors. 91st Annual Meeting of the American Ceramic Society, Indianapolis, 23–27 April 1989. In *Ceramic Dielectric Compositions, Processing and Properties, Ceramic Transactions*, Vol. 8, ed. Hung C. Ling & Man Yan. The American Ceramic Society, Westerville, Ohio, USA, 1990.
2. Haussonne, J. M., Michel, C., Le Cun, M., Boterel, F., Desgardin, G., Bourdois, P. & Raveau, B., Maîtrise de la synthèse de pérovskites au plomb pour condensateurs céramiques. In *Proceedings of the 2nd International Conference on Passive Components*, Paris, November 1987, pp. 179–83.
3. Haussonne, J. M., Le Cun, M., Bourdois, P. & Desgardin, G., Relaxor materials owning reproducible very high dielectric constants, and their behaviour under a DC bias field. 1st Conference of the European Ceramic Society, Maastricht, 18–23 June 1989. In *Euro-Ceramics*, Vol. 2. Elsevier Applied Science, London, pp. 2.277–2.282.

4. Krainik, N. N., Isupov, V. A., Bryzhina, M. F. & Agranovskaya, A. I., Crystal chemistry of ferroelectrics with the structural type tetragonal tungsten bronze (TTB). *Soviet Physics Crystallography*, **9** (1964) 281.
5. Ainger, F. W., Bickley, W. P. & Smith, G. V., The search for new ferroelectrics with the tetragonal tungsten bronze structure. *Proc. Brit. Ceram. Soc.*, **18** (1970) 221–37.
6. Scott, B. A., Giess, E. A., Burns, G. & O'Kane, D. F., Alkali rare earth niobates with the tungsten bronze type structure. *Mat. Res. Bull.*, **3** (1968) 831–42.
7. Magneli, A., Crystal structure of tetragonal potassium tungsten bronze (TTB). *Arkiv Kemi*, **1** (1949) 213–21.
8. Composition céramique à constante diélectrique élevée. French Patent No. 89 03 746, 22 March 1989.
9. Boufrou, B., Desgardin, G. & Raveau, B., The tetragonal tungsten bronze niobate $K_{0.2}Sr_{0.4}NbO_3$ (KSN): a new based material for capacitors with flat curves. In *Annual Meeting of the American Ceramic Society, Extended Abstracts of the Electronic Division*, Dallas, 22–26 April 1990, Paper 86-E-90.
10. Boufrou, B., Desgardin, G. & Raveau, B., Nouveaux diélectriques à haute constante diélectrique et courbe plate à base de $K_2Sr_4Nb_{10}O_{30}$. In *Proceedings of the Third Meeting Technologie des Céramiques pour l'Electronique et l'Electrotechnique (SEE)*, Lannion, 14–15 May 1990. Société des Electriciens et des Electroniciens, Paris, pp. AII1–AII6.
11. Herve, A., Haussonne, F. J. M. & Desgardin, G., Type I dielectric ceramics with relaxors. In *Annual Meeting of the American Ceramic Society, Extended Abstracts of the Electronic Division*, Dallas, 22–26 April 1990, Paper 85-E-90.
12. Desgardin, G., Halmi, M., Haussonne, J. M. & Raveau, B., Nouveaux matériaux diélectriques à base de pérovskites au plomb pour condensateurs multicouches de type II. *J. Phys. Coll. CI, Suppl. No. 2*, **47** (1981) CI 889.
13. Halmi, M., Desgardin, G. & Raveau, B., Low temperature sintered lead niobates-based ceramics of high dielectric constants. *Mat. Lett.*, **5** (1987) 103.
14. Haussonne, J. M., Regreny, O., Lostec, J., Desgardin, G., Halmi, M. & Raveau, B., Sintering of various perovskites with lithium salts. In *6th CIMTEC World Congress on High Tech Ceramics*, Milan, 24–28 June 1986, ed. P. Vincenzini. Elsevier, Amsterdam, 1987, pp. 1515–24.
15. Boufrou, B., Desgardin, G. & Raveau, B., The tetragonal tungsten bronze niobate $K_{0.2}Sr_{0.4}NbO_3$: a new material for capacitors with flat dielectric curves. *J. Am. Ceram. Soc.*, **74** (1991) 2809–14.
16. Pouchard, M., Chaminade, J.-P., Perron, A., Ravez, J. & Hagenmuller, P., Influence de divers types de substitutions cationiques sur les propriétés diélectriques de niobates de structure bronzes oxygénés de tungstène quadratiques. *J. Solid State Chem.*, **14** (1975) 274–82.
17. Thorel, J. & Ravez, J., Influence of cationic orders on dielectric properties of some TTB phases. *Rev. Chim. Minér.*, **24** (1987) 2881.
18. Desgardin, G., Mey, I., Raveau, B. & Haussonne, J. M., $BaLiF_3$, a new sintering agent for $BaTiO_3$-based capacitors. *Ceram. Bull.*, **64** (1985) 564.

Appendix: Classification of Dielectric Materials

The EIA specifications give the characteristics of dielectric materials:

—**Type I materials** are generally paraelectric materials. They are characterized by a close to linear variation of permittivity versus temperature. *Pxxx* or *Nxxx* have respectively a positive or a negative temperature dependence of permittivity with *xxx* in ppm/°C, while NPO is related to a non-temperature dependence. Correlated with the value of the slope of the temperature dependence, the specifications also define the values of the maximum allowed dielectric losses.

—**Type II materials**, that are generally ferroelectric materials, are characterized by an allowed temperature dependence of the permittivity in a given range of temperature. They are described by the EIA specifications by a group of two letters and one number: the first letter gives the lower limit of temperature, the following number the upper limit of temperature, and the last letter the allowed relative variation of permittivity in this range of temperature. As examples, the most popular materials have characteristics summarized in Table A1:

Table A1. Characteristics of the most popular dielectric ceramic materials

EIA designation	*Lower temperature* (°C)	*Upper temperature* (°C)	*Relative permittivity* (%)
Z5U	+10	+85	+22/−55
Y5V	−30	+85	+22/−82
X7R	−55	+125	±15